FR2198-20

15 October 1993

FATIGUE IN SINGLE CRYSTAL NICKEL SUPERALLOYS

Interim Technical Report

D. P. DeLuca
Prinicpal Investigator

Charles Annis
Program Manager

UNITED TECHNOLOGIES PRATT&WHITNEY
P.O. Box 109600
West Palm Beach, FL 33410-9600
(407)796-6565
Government Engines and Space Propulsion

15 October, 1993

Period of performance
16 September 1991 through 15 October 1993

Contract N00014-91-C-0124

Prepared for:
Dr. A. K. Vasudevan, Scientific Officer

Office of Naval Research
Department of the Navy
800 N. Quincy Street
Arlington, Va 22217-5000

I: Introduction

The following paragraphs provide a narrative summary of this program to date. Background information, including the Introduction and Program Objective and Program Organization, follows this section.

Program Synopsis

We described (in our December 1991 monthly report, FR-21998-02) a stress intensity (K) dependent fatigue crack growth mode transition, environmentally activated by high pressure hydrogen (a low energy fracture mode under high energy conditions) that could result in a 100X increase in fatigue crack propagation rate. We defined a microstructural modification that resulted in a 4X decrease in fatigue crack propagation rate under the most severe operating conditions (FR-21998-08).

We conducted temperature gradient and frequency gradient tests (FR-21998-13 and 21998-14) and documented fracture mode transitions as a function of temperature and energy input rate.

Through fundamental understandings such as these there exists a potential for improved damage tolerance which could, for example, by invoking a high energy fracture mode under low energy conditions resulting in an (observed) 10X decrease in fatigue crack propagation rate at a given condition. This behavior seems to be generic and therefore applicable to other alloy systems of interest to the Navy beyond flight materials.

We provided size versus frequency of occurrence plots for the principal IMQ (intrinsic material quality) defects in PWA 1480 and PWA 1484. The bulk of this data was obtained from fatigue failure origins making the data extremely valuable. We also provided distributions obtained via metallographic sections for comparison and statistical investigator T. Watkins produced a correction factor to equate the two different types of distributions.

We submitted nineteen monthly progress reports and published one paper, "Markov Fatigue in Single Crystal Airfoils," by Charles Annis and Daniel P. DeLuca, presented at the ASME International Gas Turbine and Aeroengine Congress and Exposition, Cologne, Germany, June 1-4, 1992.

II. Introduction and Program Objective

This program investigates the seemingly unusual behavior of single crystal airfoil materials. The fatigue initiation processes in single crystal (SC) materials are significantly more complicated and involved than fatigue initiation and subsequent behavior of a (single) macrocrack in conventional, isotropic, materials. To understand these differences it is helpful to review the evolution of high temperature airfoils.

Characteristics of Single Crystal Materials

Modern gas turbine flight propulsion systems employ single crystal materials for turbine airfoil applications because of their superior performance in resisting creep, oxidation, and thermal mechanical fatigue (TMF). These properties have been achieved by composition and alloying, of course, but also by appropriate crystal orientation and associated anisotropy.

Early aeroengine turbine blade and vane materials were conventionally cast, equiaxed alloys, such as IN100 and Rene'80. This changed in the late 1960s with the introduction of directionally-solidified (DS) MAR-M200+Hf airfoils. The DS process produces a <001> crystallographic orientation, which in superalloys exhibits excellent strain controlled fatigue resistance due to its low elastic modulus. The absence of transverse grain boundaries, a 60% reduction in longitudinal modulus compared with equiaxed grains, and its corresponding improved resistance to thermal fatigue and creep, permitted significant increases in allowable metal temperatures and blade stresses. Still further progress was achieved in the mid-1970s with the development of single crystal airfoils[1].

The first such material, PWA 1480, has a considerably simpler composition than preceding cast nickel blade alloys because, in the absence of grain boundaries, no grain boundary strengthening elements are required. Deleting these grain boundary strengtheners, which are also melting point depressants, increased the incipient melt temperature. This, in turn, allowed nearly complete solutioning during heat treatment and thus a reduction in dendritic segregation. The absence of grain boundaries, the opportunity for full solution heat treatment, and the minimal post-heat treat dendritic segregation, result in significantly improved properties as compared with conventionally cast or directionally solidified alloys. Single crystal castings also share with DS alloys the <001> crystal orientation, along with the benefits of the resulting low modulus in the longitudinal direction.

Pratt & Whitney has developed numerous single crystal materials. Like most, PWA 1480 and PWA 1484 are strengthened cast mono grain nickel superalloys based on the Ni-Cr-Al system. The bulk of the microstructure consists of approximately 60% by volume of cuboidal precipitates in a matrix. The precipitate ranges from 0.35 to 0.5 microns and is an ordered Face Centered Cubic (FCC) nickel aluminide compound. The macrostructure of these materials is characterized by parallel continuous primary dendrites spanning the casting without interruption in the direction of solidification. Secondary dendrite arms (perpendicular to solidification) define the interdendritic spacing. Solidification for both primary and secondary dendrite arms proceeds in <001> type crystallographic directions. Undissolved eutectic pools and associated microporosity reside throughout the interdendritic areas. These features act as microstuctural discontinuities, and often exert a controlling influence on the fatigue initiation behavior of the alloy. Also, since the eutectics are structurally dissimilar from the surrounding matrix their fracture characteristics will differ.

---

[1] Gell, M., D. N. Duhl, and A. F. Giamei, 1980, "The Development of Single Crystal Superalloy Turbine Blades," *Superalloys* 1980, proceedings of the Fourth International Symposium on Superalloys, American Society for Metals, Metal Park, Ohio, pp. 205-214

Single Crystal Fatigue

The fatigue process in single crystal airfoil materials is a remarkably complex and interesting process. In cast single crystal nickel alloys, two basic fracture modes, crystallographic and non-crystallographic, are seen in combination. They occur in varying proportions depending upon temperature and stress state. Crystallographic orientation with respect to applied load also affects the proportion of each and influences the specific crystallographic planes and slip directions involved. Mixed mode fracture is observed under monotonic as well as cyclic conditions.

Single crystal turbine blades are cast such that the radial axis of the component is essentially coincident with the <001> crystallographic direction which is the direction of solidification. Crystallographic fracture is usually seen as either octahedral along multiple (111) planes or under certain circumstances as (001) cleavage along cubic planes.

Non-crystallographic fracture is also observed. Low temperatures favor crystallographic fracture. At higher temperatures, in the 427C range, small amounts of non-crystallographic propagation have the appearance of transgranular fatigue in a related fine grain equiaxed alloy. Under some conditions, this propagation changes almost immediately to the highly crystallographic mode along (111) shear planes, frequently exhibiting prominent striations emanating from the fatigue origin and continuing to failure in overstress. Under other conditions the non-crystallographic behavior can continue until tensile failure occurs. At intermediate temperatures (around 760C) non-crystallographic propagation is more pronounced and may continue until tensile overload along (111) planes occurs, or may transition to subcritical crystallographic propagation. At 982C, propagation is almost entirely non-crystallographic, similar to transgranular propagation in a polycrystal.

Damage Catalogue

This program will identify and compile descriptions of the fracture morphologies observed in SC airfoil materials under various combinations of temperature and stress associated with advanced Navy aeropropulsion systems. We will suggest fatigue mechanisms for these morphologies and catalogue them as unique damage *states*. Most testing will be accomplished under ancillary funding, and therefore be available to this effort at no cost. The work is organized into four tasks, which are described in the following paragraphs.

III. Program Organization

The program is structured into four tasks, three technical and one reporting. The individual tasks are outlined here.

Task 100 - Micromechanical Characterization
This task will define the mechanisms of damage accumulation for the various types of fracture observed in single crystal alloys. These fracture characteristics will be used to establish a series of Damage States which represent the fatigue damage process. The basis for this investigation

will be detailed fractographic assessment of failed laboratory specimens generated in concurrent programs. Emphasis will be on specifically identifying the micromechanical damage mechanisms, relating them to a damage state, and determining the conditions required to transition to an alternate state.

Task 200 - Analytical Parameter Development

This task will extend current methods of fatigue and fracture mechanics analysis to account for microstructural complexities inherent in single crystal alloys. This will be accomplished through the development of flexible correlative parameters which can be used to evaluate the crack growth characteristics of a particular damage state. The proposed analyses will consider the finite element and the hybrid Surface-Integral and Finite Element (SAFE) methods to describe the micromechanics of crack propagation.

Task 300 - Probabilistic Modeling

This task will model the accumulation of fatigue damage in single crystal alloys as a Markov process. The probabilities of damage progressing between the damage states defined in Task 100 will be evaluated for input into the Markov model. The relationship between these transition probabilities and fatigue life will then be exploited to establish a model with comprehensive life predictive capabilities.

Task 400 - Reporting

Running concurrently with the analytical portions of the program, this task will inform the Navy Program Manager and Contracting Officer of the technical and fiscal status of the program through R&D status reports.

IV. Technical Progress

4.1.1: Micromechanical Characterization

Initially, our efforts were concentrated on identifying and characterizing numerous damage states in both PWA 1480 and PWA 1484 + HIP. Our approach has been to build on accepted micro mechanisms and classical dislocation theory for the deformation process in two phase FCC systems and to propose new hypotheses on the sequential nature of the accumulation and dissipation of strain energy. Sources for this study included specimen fractures and test data produced under past and present NASA, Air Force and P&W IR&D programs.

4.1.2: Micromechanical Fracture Modes/Transitions

Our objective has been to identify the micromechanical damage states comprising the fatigue and fracture process. Our approach has been to conduct a detailed fractographic and metallographic analysis of the study alloys. This effort paid particular attention to energy

dependent (ΔK) microscopic fracture mode transitions and any fracture details that serve as indicators of an incipient transition. These details can form a basis to predict the probability of a state transition, a principal requirement of the Markov transition probability matrix. Microscopic fracture modes and transition behavior are of critical importance because they affect fatigue crack initiation and propagation. From the perspective of the Markov paradigm these transitions may be considered as bridging sequential damage states (or sub states), which may, under a particular set of circumstances or conditions, lead to an absorbing state such as failure. These indicators are in the form of condition (temperature or stress intensity for example) dependent fracture details on the γ' precipitate level. Further, these fracture modes are phase specific in some cases (i.e.., dissimilar modes can exist simultaneously in various constituents of the microstructure). Some phases lead others in going through a transition and therefore represent indicators.

In order to conduct this type of investigation it has been necessary to develop some new techniques for analysis and characterization of fracture surfaces. This work was carried out from the macroscopic level to 300,000 X via optical techniques, scanning electron microscopy (SEM), replica and transmission electron microscopy (TEM) and scanning/transmission electron microscopy (STEM).

By the adaptation of the Philips CM-20 STEM for use as a fracture analyses tool, fractographic images in excess of 100,000 *X* were produced. Magnifications in this range were necessary to resolve the micromechanisms of fracture on the $\gamma-\gamma'$ interface level.

Graphic representations of particular fracture modes were assembled via Unigraphics Shaded-Solid Modeling. The models are three dimensional and can be rotated to provide needed views of a particular fracture. They aided in the process of understanding and describing crack tip / microstructure interactions.

A further development identified an automated method of obtaining both graphic and statistical assessments of micro mechanical transition indicators. The Rodenstock Laser Imaging Profilometer is intended to assess optically surface roughness via a laser stylus. For the purposes of this program, the instrument represents a scanning laser micro analyzer with statistical analysis capabilities. "Quantitative fractography" (Underwood) can provide a mathematical "signature" of a particular fracture mode or transition useful in assessing the stochastic component of a *K*-dependant transition.

A description of a stress intensity induced fracture mode transition and the methods of analysis we have described are provided in the following figures.

The eutectic ($\gamma-\gamma'$) exhibits an energy dependent sequence of microscopic fracture modes similar to those observed in the bulk microstructure but at a slightly different energy input level (ΔK). This causes it to become a preferential fatigue crack initiation site under certain circumstances and also (by definition) to go through a *K* dependent fracture transition at a slightly different stress intensity than the bulk of the microstructure. As such, it can function as a barometer for an impending fracture mode transition.

The transition that revealed this behavior was observed in PWA 1480 at room temperature by Telesman[2] in a load shedding fatigue crack growth test. The transition was shown to repeat in reverse order upon subsequent cycling at constant load. The test was repeated at P&W.
The PWA 1480 room temperature threshold crack growth evaluation was conducted in a decreasing-K mode (negative K-gradient). A fracture mode transition occurred at approximately 8-10 MPa $\sqrt{m}$ accompanied by a marked change in growth behavior. A plot of the test results is shown in Figure 1. The mode change is shown schematically in Figure 2. The transition was from microscopic octahedral, (111) crystallographic fracture on the level of the cuboidal γ' precipitate, to failure at the $\gamma-\gamma'$ interface (referred to as decohesion or interphase fracture). The transition occurred initially in the eutectic $\gamma-\gamma'$ shown before and after transition (Figure 3).

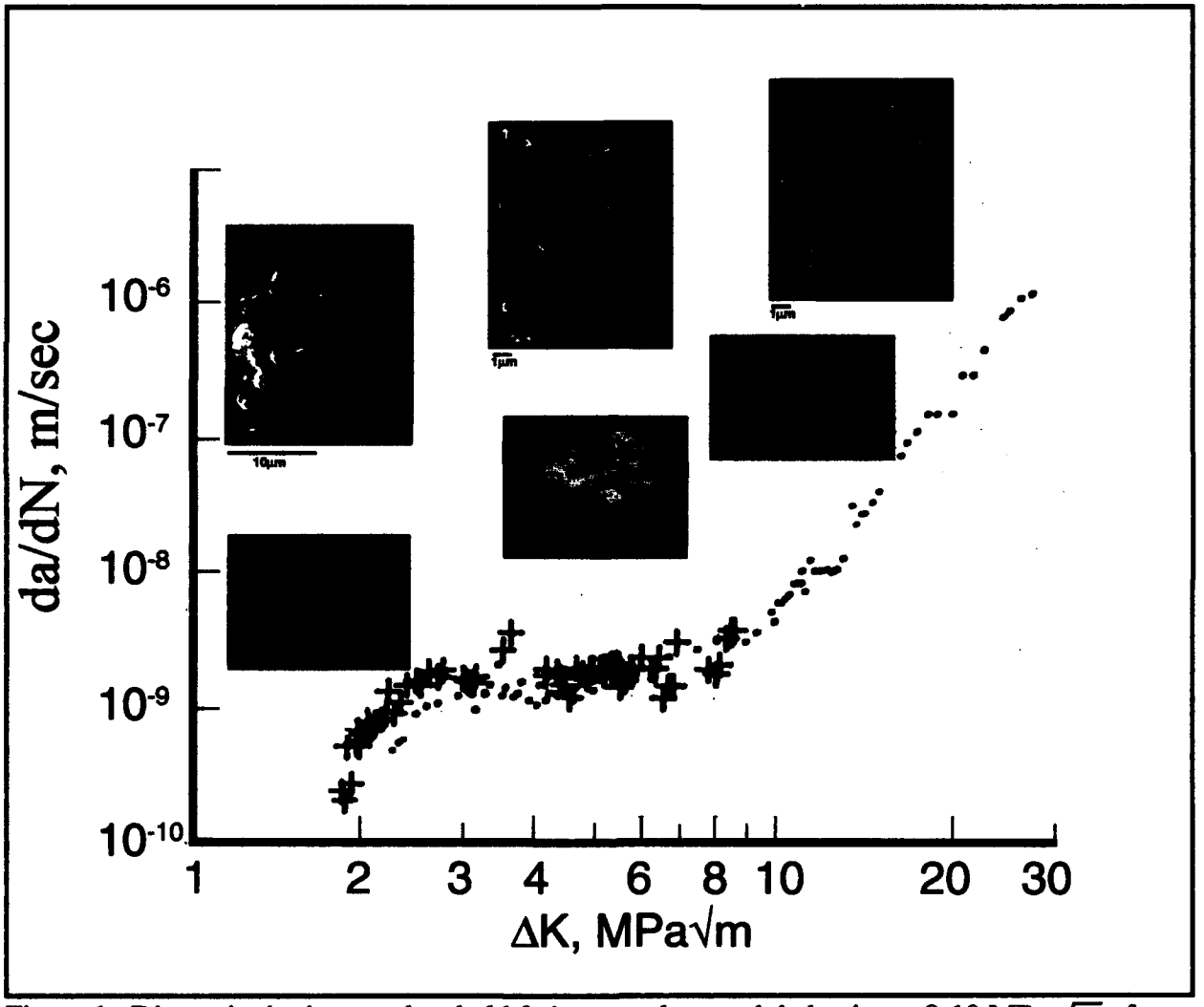

Figure 1. Discontinuity in near threshold fatigue crack growth behavior at 8-10 MPa $\sqrt{m}$ for PWA 1480 at room temperature. A transition in the operative fatigue crack growth mode resulted in this behavior.

---

[2] Telesman and Ghosn, 1989, "The Unusual Near-Threshold FCG Behavior of a Single Crystal Superalloy and the Resolved Shear Stress as the Crack Driving Force," *Engineering Fracture Mechanics*, Vol. 34, No. 5/6, pp. 1183-1196.

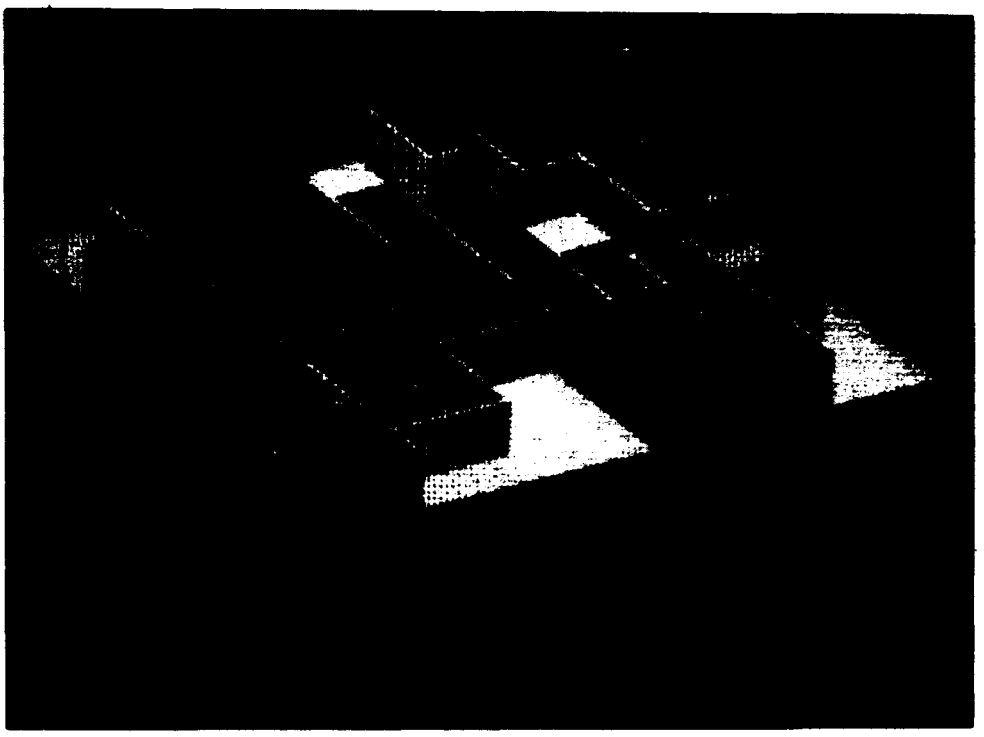

Figure 2. Shaded-solid model of the near threshold fracture mode shown in the previous figure. The cuboidal γ precipitates are approximately 0.5 - 1.0 microns square, the γ' matrix is approximately 0.03 microns wide.

Fracture surfaces for the two modes are shown in Figure 4. Details of a decohesion failure in PWA 1484 are shown in Figure 5. A representative laser scan of the transition zone for this type of fracture sequence is displayed in a 3 axis representation in Figure 6. The data from the profile plot has been converted to a topographical contour plot in Figure 7.

Elevated temperature tests of this type were planned to begin in a separate effort and would provide subjects for similar analysis. In the interim period we focused on the micromechanics of fatigue crack initiation. In an effort to make this narrative loosely chronological we now shift our discussion to the study of fatigue crack initiation. We will return to the micromechanics of fracture presently.

4.2: The Micromechanics of Fatigue Crack Initiation

Identification of the micromechanisms of initiation is an important part of this effort. Fatigue life is defect driven and our study has focused on intrinsic material quality defects (IMQ). We feel that the quantitative, qualitative and micromechanical characterization of these defects parallels (on the initiation side) our efforts to identify and categorize additional damage states (on the fracture side.)

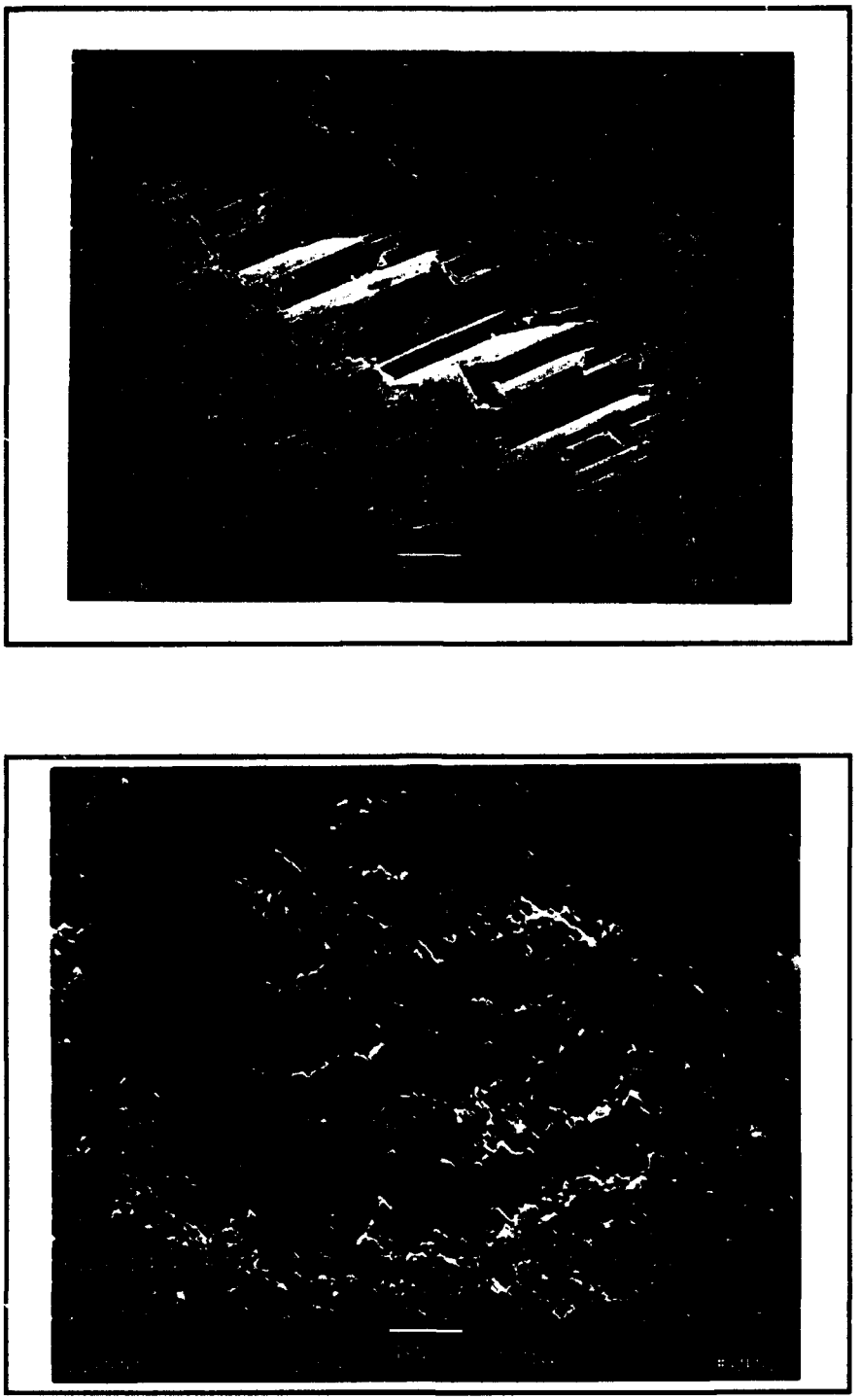

Figure 3: Microscopic fracture modes observed in eutectic $\gamma-\gamma'$ in PWA 1480 at room temperature. Top is seen in Region II FCG, where it is synchronous with that observed in the bulk of the microstructure (the cuboidal $\gamma-\gamma'$ matrix structure). Bottom is an interlamellar fracture asynchronous in the near threshold region prior to complete transition of the bulk of the microstructure

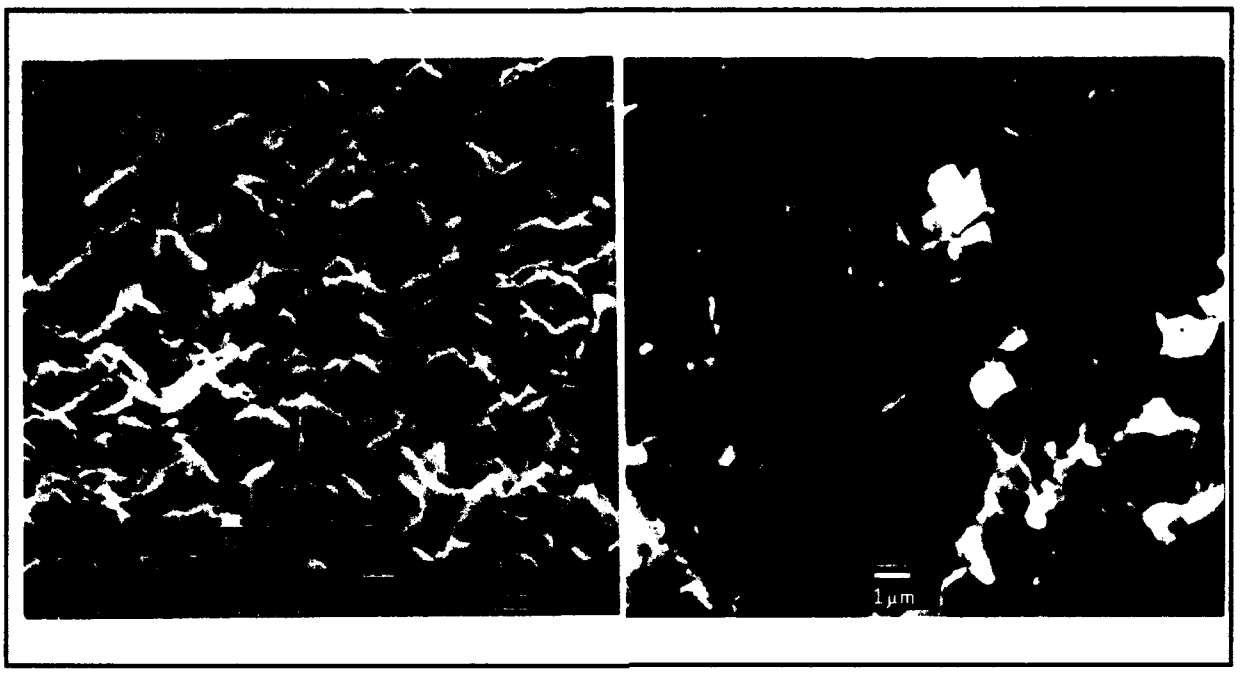

Figure 4. A comparison of local octahedral (left) and $\gamma-\gamma'$ phase decohesion (right). Local octahedral fracture characterizes room temperature region II fatigue crack growth. Inter-phase fracture is common to both room temperature threshold behavior in air and regions I through III fatigue growth in a high pressure hydrogen environment.

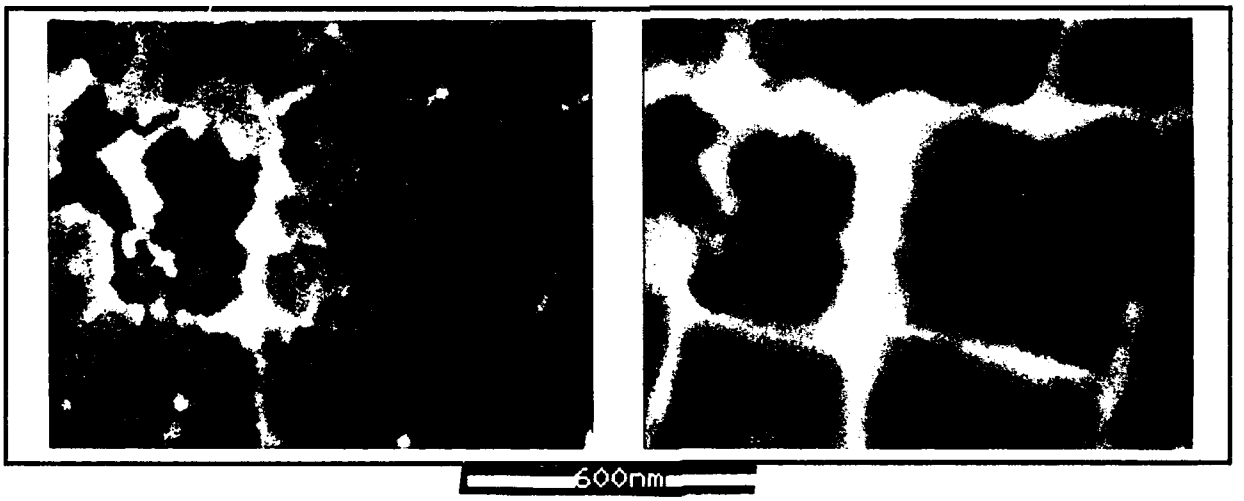

Figure 5. Inter-phase fracture in PWA 1484 from a fatigue test in 5000 psi gaseous hydrogen simulating a rocket environment. The fracture is imaged in secondary emission (left) for topographical contrast and suggests octahedral fracture of the $\gamma-\gamma'$ matrix surrounding the cubic precipitates. The backscatterd electron image (right) delineates the areas of the γ matrix on the fracture surface.

RODENSTOCK METROLOGY RM600

Display	
Points	7158
Scans	50
Display range	.5000 mil
Measurement range	30 µm
Table speed	0.079 in/min
Y Length	0.020 in
X Length	0.004 in
Name of data set	DAN0

Remarks ..... rear scan
Examiner ..... STETSON
Date ..... 13.12.91 Version: 2.50E02

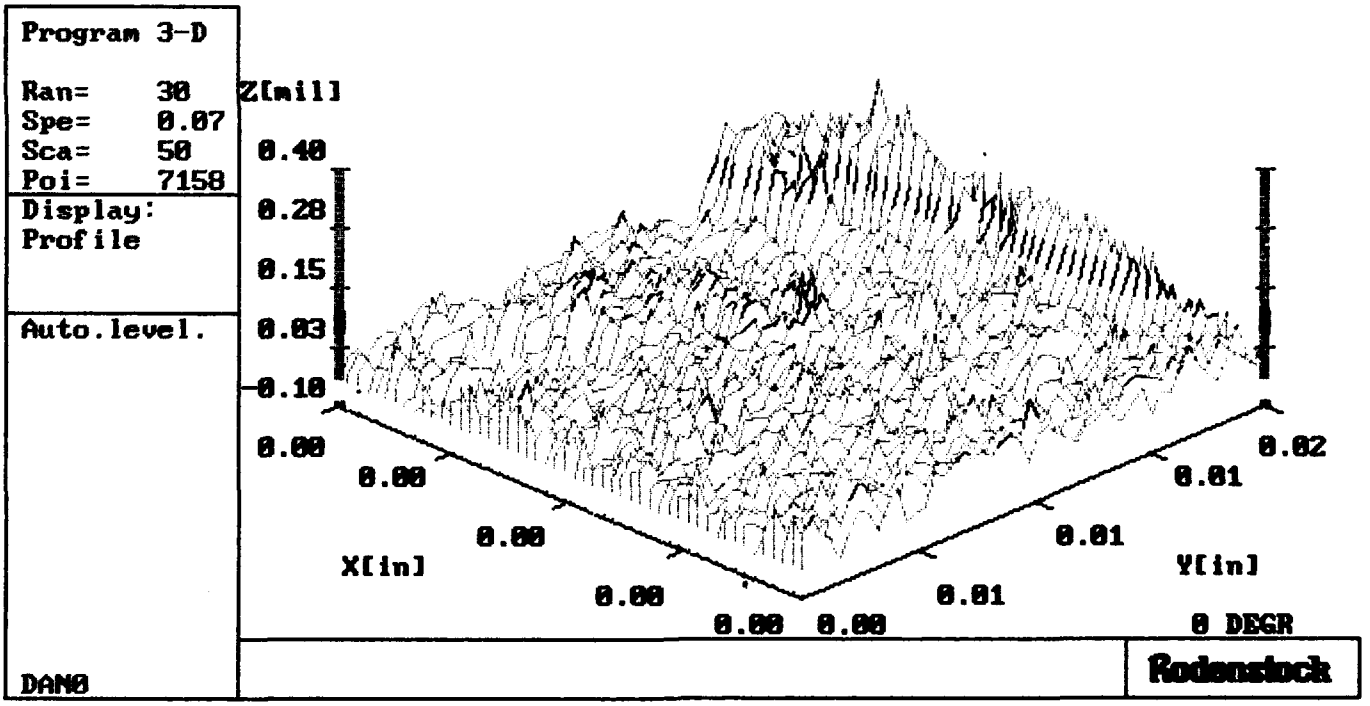

Figure 6. Profile image of transition zone from decohesion to local octahedral fracture.

RODENSTOCK METROLOGY RM600

Display	
Points 7158	
Scans 50	
Display range ..... .5000 mil	
Measurement range ..... 30 µm	
Table speed ..... 0.079 in/min	
Y Length ..... 0.020 in	
X Length ..... 0.004 in	
Name of data set DAN0	
Remarks ..... rear scan	
Examiner ..... STETSON	
Date 13.12.91	Version: 2.50E02

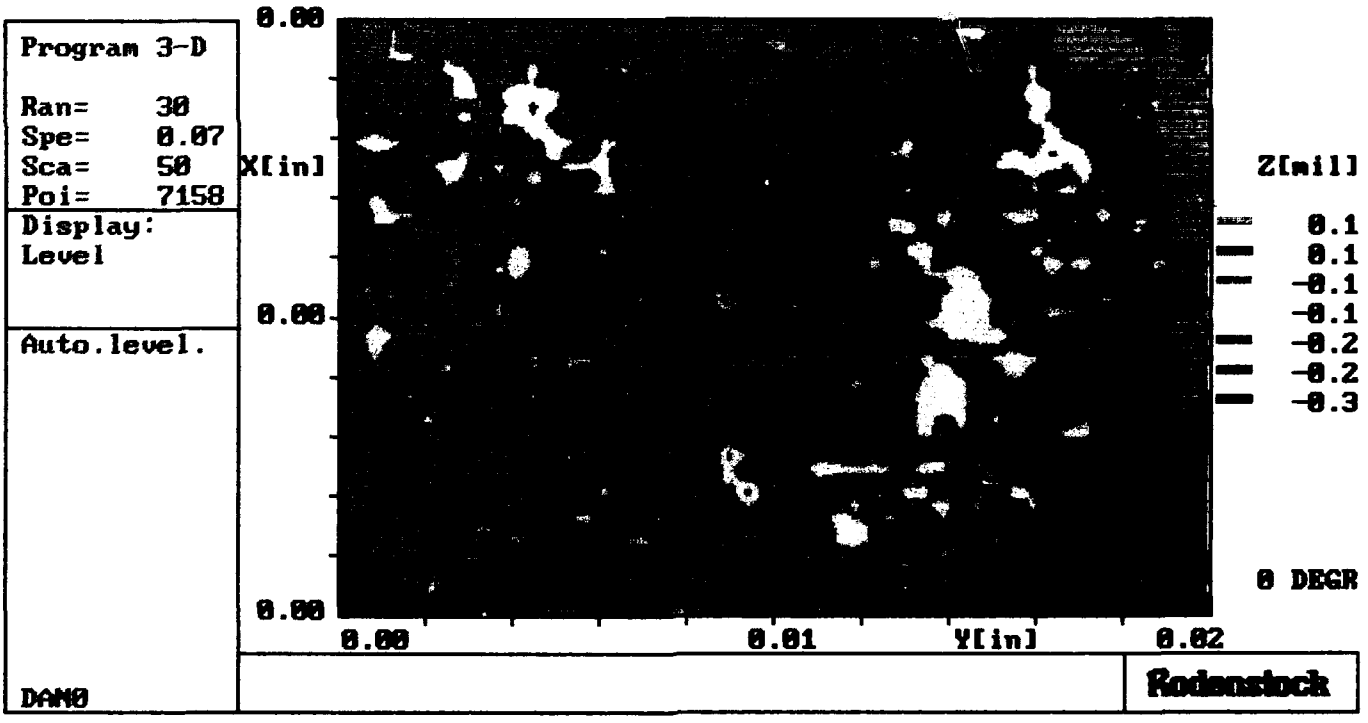

Figure 7. Surface contour of transition zone imaged in previous figure.

To characterize the incubation phase of the fatigue process it is necessary to consider the nature of the various sources of fatigue crack initiation. Fatigue cracks typically initiate at defects. Defects can be thought of as falling into two basic types, those of intrinsic material quality (IMQ) and those stemming from deviant material. IMQ defects are a normal feature of an alloy and are included in material capability curves and empirically based life prediction systems. There are established tolerance limits on these.

Rejectable defects are defects stemming from some deviation in material quality that exceeds specified limits. They are not included in alloy capability curves. Within the scope of this program it is practical to make some observations regarding such details as threshold size for initiation, size probability density and the micromechanics that characterize a particular defect species. A micromechanical assessment of incubation time could allow the prediction of IMQ defect driven initiation life based on the energy imparted to the microstructure during cyclic loading providing a means of assessing the transition probability from the undamaged state.

4.2.1: Temperature Dependent IMQs

Identifying and cataloging temperature dependent defects is important to fatigue life modeling. Recent SEM review of PWA 1484 fractures produced at 800F, shows secondary crack formation (figure 8) at the interface between the eutectic phase and the bulk microstructure. This is an indication that the eutectic is not a benign defect. Low temperature origins are frequently seen at small carbides in PWA 1480. Elevated temperature initiations stem from microporosity in the absence of HIP in PWA 1480 and PWA 1484. The fact that the eutectic "phase" can become a fatigue crack initiator at 800F indicates the need to determine the temperature range where it is an active defect. Then, a size distribution and threshold size evaluation is needed. Historical 600F PWA 1480 fractures were examined specifically for additional evidence of this phenomenon. These fractures show an extreme case of this mechanism where the phase has experienced decohesion from the microstructure bulk, i.e.. pulled out.

There are insufficient archival specimen fractures available to properly define the activation temperature range for eutectic pullout. A potential method to determine the temperature limits would be a constant K crack growth test where temperature is varies from T_1 to T_2 over time. Analysis of the fracture surface then yields the temperature range favoring pullout.

The fracture surface may also provide other information about critical dislocation density at the eutectic/bulk interface. A compact tension crack growth specimen provides sufficient fracture area to obtain specimens of the fracture surface for thin foil transmission electron microscopy. This permits comparative analysis of dislocation structures associated with eutectic pullout versus fracture.

4.2.2: Probabilistic IMQ Methodology

Other defects that were assessed were the tantalum carbide (TaC) phase present in current chemistry PWA 1484 and microporosity found in non-hipped PWA 1484 and PWA 1480. To assess these defects from a quantitative standpoint, statistical frequency-of-occurrence

distributions for size versus frequency of occurrence are needed. Numerous failed LCF specimens (archival) have provided this information.

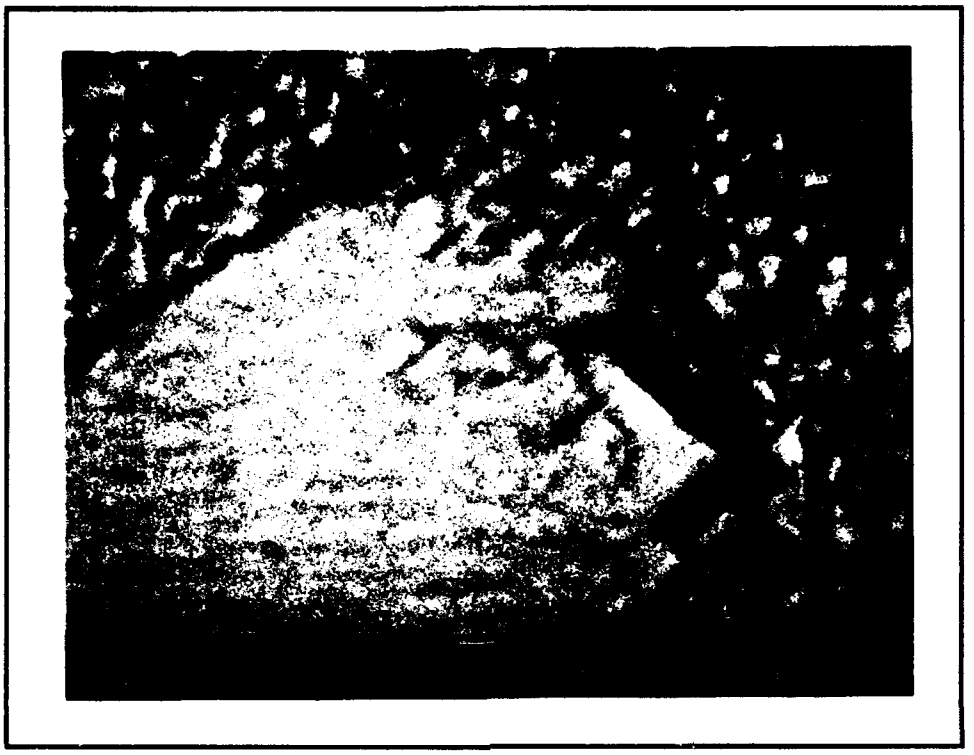

Figure 8: Secondary crack formation of the eutectic/bulk microstructure interface in PWA 1484 plus HIP at 800F.

The distributions for microporosity from fatigue failure origins in PWA 1480 and non hip PWA 1484 are shown in Figure 9. Since these observations were obtained from fatigue fracture surfaces at failure origins, the distributions provide an indication of the defect threshold size (the minimum size observed at a fatigue origin). PWA 1480 and PWA 1484 are plotted as a single population. An analysis of variance and F-test showed no statistically significant difference between the means and variances of the two populations when treated separately.

4.2.3: Microstructural Image Analysis

A recent increase in the carbon content of PWA 1484 to enhance its castability has changed the TaC distribution. Insufficient fractures exist for the current chemistry PWA 1484 to provide a distribution based on fatigue crack initiation sites. In this case distributions were developed via metallographic image analysis. The specimens also produced distributions for the eutectic phase and porosity in PWA 1480. These distributions for TaC and eutectics are shown in figure 10. The distribution for porosity from sectioning PWA1480 is shown in figure 11.

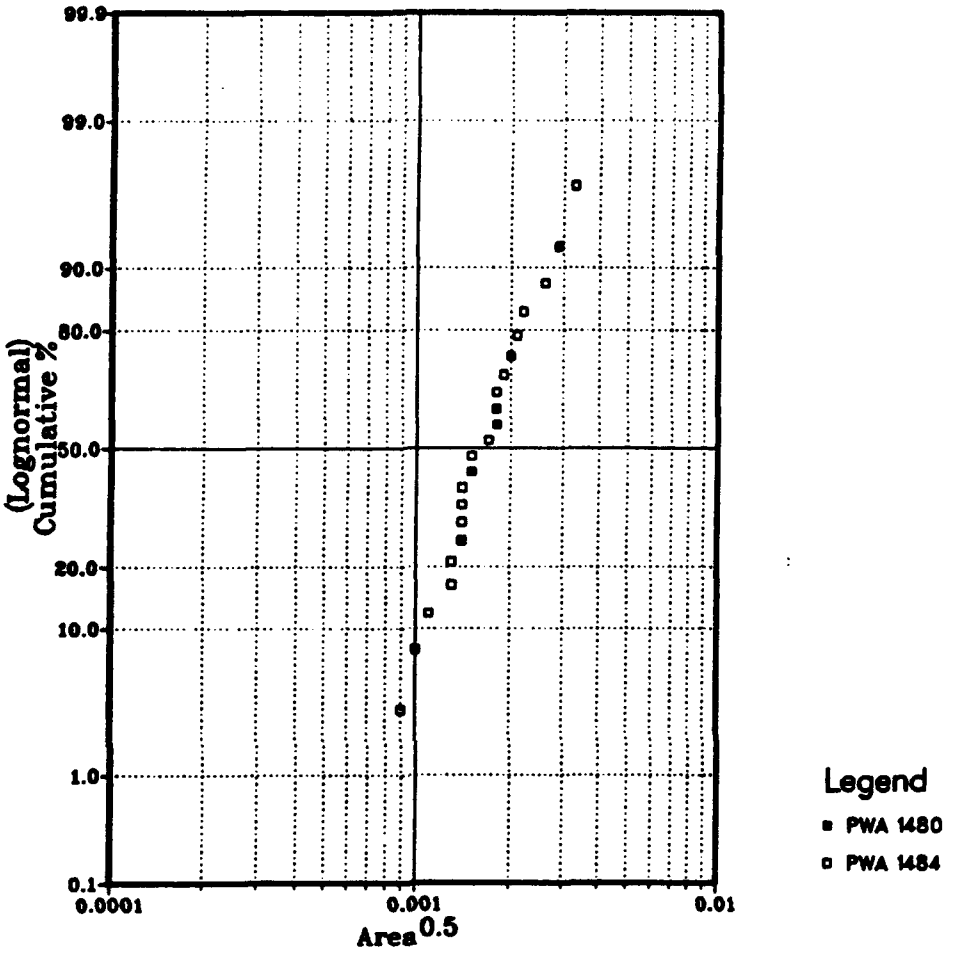

Figure 9: Size vs. Frequency-of-Occurrence for Microporosity in PWA 1480 and PWA 1484.

Probabilistic Modeling (Task III)

The temperature dependency of the eutectic phase as a fatigue crack initiator complicates the approach to a probabilistic assessment of IMQ defects since the resulting statistical distribution may be influenced by the test condition. Ideally, IMQ populations would be constant regardless of conditions, existing as a function of only the material chemistry and processing. Potential dependency on test conditions is under investigation. The probability of activation of a condition dependent defect needs to be included in Markov transition probabilities (or any probabilistic system and is not current practice).

Also to be addressed is the relationship between distributions of IMQs obtained from metallographic and ex post facto fracture specimen analysis. In comparing the distributions from figures 9 and 11, it appears that a model relating the two distributions could be developed. Should this be the case, metallographic sectioning results might be used to replace the extensive (and expensive) database usually developed from failed fatigue specimens.

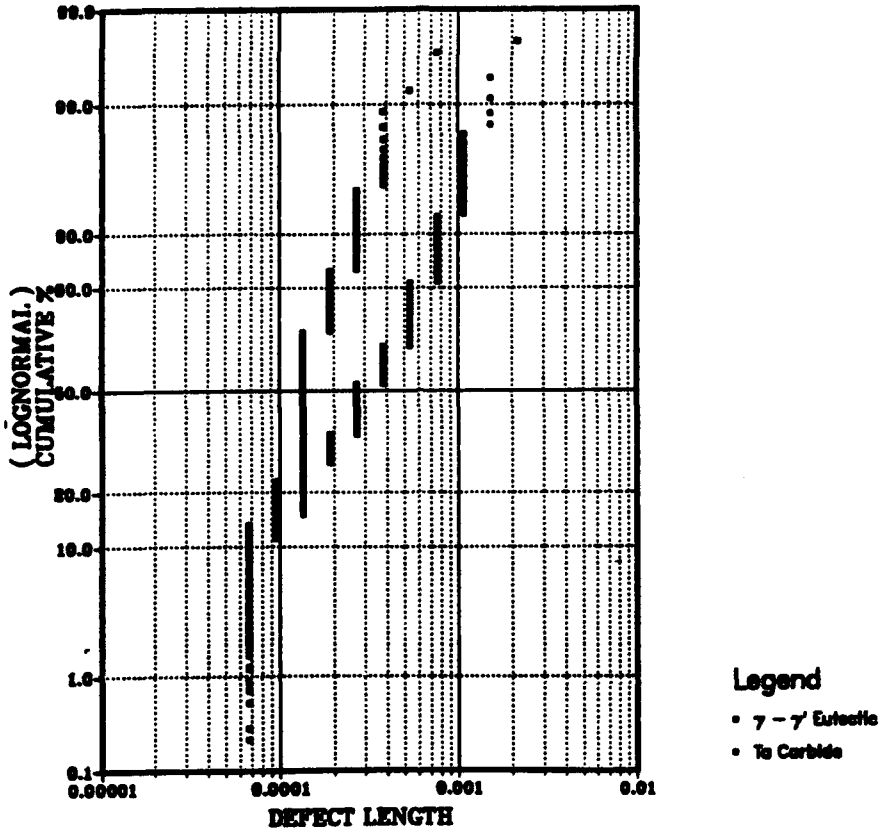

Figure 10: Eutectic and Tantalum Carbide distributions for PWA 1484 obtained from metallographic sectioning

4.2.4: IMQ Severity

The threshold size for a TaC to initiate a fatigue crack was estimated based on the minimum size origin present (Figure 12) in the available fracture data base. TaC defects fracture as opposed to decohesion and recent study suggests that this may be a result of slip band impingement. This too is associated with dislocation buildup at the defect/bulk microstructure interface. The determining factors affecting decohesion versus fracture are of some importance.

The difference may be related to the relative defect morphologies. Qualitatively, the TaC is typically seen as a "Chinese Script" type carbide (Figure 13) while the eutectic phase (Figure 14) is comparatively spherical or ovoid in shape. The script shape would tend to be interlocked in the matrix while the eutectic phase is free to pull out cleanly without fracturing. The relative

physical properties of the two phases would also favor fracture of TaC since the eutectic phase is considerably more ductile.

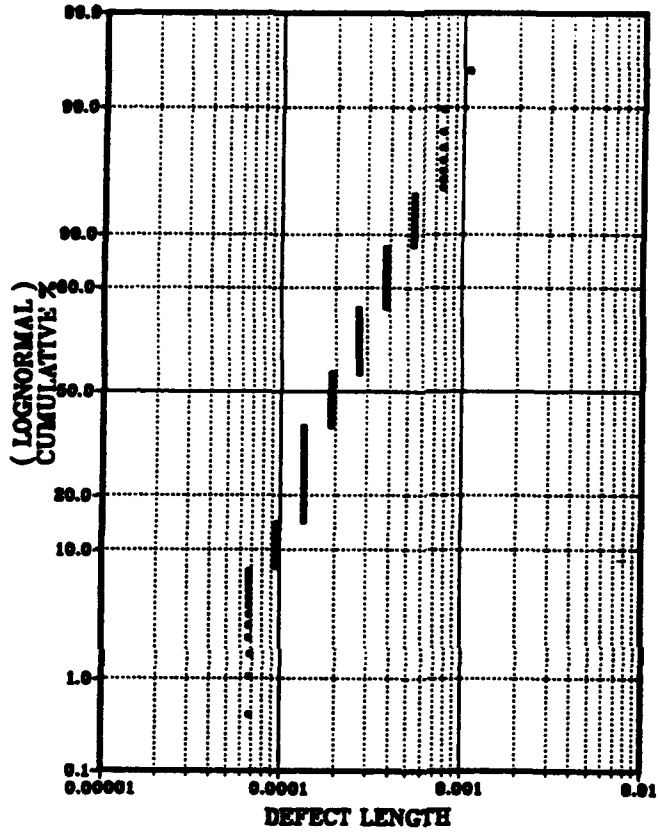

Figure 11: Porosity distribution for PWA 1480 obtained from metallographic sectioning

In addition, a fractographic review of available fractures was conducted. Based on that limited data base it appears that the threshold size for eutectic pullout is similar to the previously shown distribution for porosity. An example of a fatigue initiation from eutectic pullout is shown (Figure 15). Upon eutectic pullout a void with morphology similar to a pore develops (Figure 16). In contrast the TaC is a low ductility defect prone to brittle fracture initiating sharp microcracks in the bulk microstructure.

4.2.5: Environmental Effects

We have investigated the effects of pernicious environments such as hydrogen. The micromechanics of fatigue and fracture in high pressure hydrogen parallel air behavior in some

respects and can provide perspective in the area of Initial Material Quality (IMQ) defect activation. Our interest in defect activation stems primarily from experience with PWA 1480, the current bill of material alloy for the NASA Space Shuttle Main Engine Alternate Turbopump Design (SSME-ATD). This SSME-ATD application employs 1st and 2nd stage turbine blades of PWA 1480 in both the high pressure fuel and oxidizer turbopumps.

Figure 12: A secondary LCF initiation at a surface connected TaC approximately .00025" wide. (*1000X*)

Figure 13. A qualitative perspective on a TaC observed at a fatigue origin. This type of carbide morphology is commonly referred to as a "Chinese Script" carbide. (*500X*)

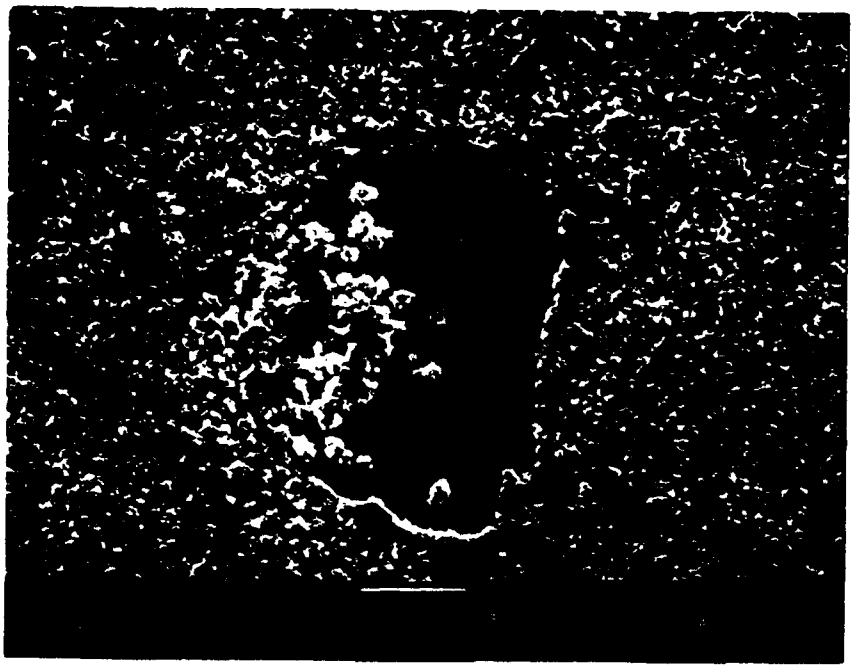

Figure 14. A PWA 1480 fracture showing the eutectic phase. The defect morphology is considerably different than that of TaC.

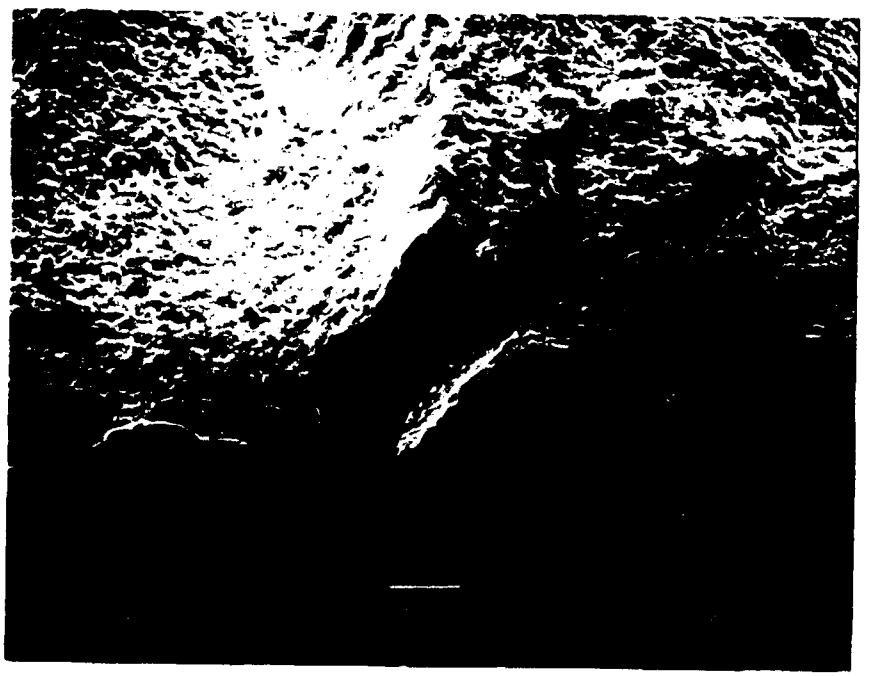

Figure 15: An Initiation Point From Eutectic Decohesion.

Previously we introduced the concept of a condition dependent defect species; we identified the $\gamma-\gamma'$ eutectic as a temperature dependent IMQ defect. The activation mechanism is likely to be differential thermal expansion resulting in a transient condition of high misfit. The resultant fatigue crack initiation mechanism is pullout of the eutectic from the microstructure at large and subsequent void formation with an associated stress concentration. This mechanism is more akin to that of initiation at a micropore and the overall severity appears similar. An observation that

provides an illustrative example of the effect of defect severity (and a demonstration of how LCF behavior is strongly defect driven) follows.

Figure 16: High magnification study of eutectic pullout and two small micropores.

The eutectic can become a fatigue crack initiator in another way. In-situ high pressure (5000 psi) hydrogen testing of PWA 1480 at room temperature results in a fracture mode transition in the eutectic. Fatigue crack initiation starts at the interface between the eutectic lamella, resulting in an extremely (infinitely) sharp microcrack. This micromechanism is very different from the pullout of the entire phase from the microstructure described earlier. The severity of this newly described mechanism is extreme when we consider the effect on LCF life. Notched LCF life of PWA 1480 in room temperature high pressure hydrogen is reduced by more than an order of magnitude at 90 KSI. The elimination of the eutectic by solutioning at a higher than normal temperature mitigates the life debit. The environmental activation of this defect serves as another example of a condition dependent defect. It also demonstrates the effect of defect severity (and the value of a knowledge of micromechanics).

Interlamellar failure of the eutectic is a more sever failure mechanism than pullout of the eutectic, even though the defect species (the eutectic) is the same for both failures.

4.3: Elevated Temperature Fracture

In order to characterize elevated temperature fracture, fatigue crack growth specimens from ancillary programs were reviewed.

We used the knowledge base gained in studying low temperature fracture to develop an understanding of elevated temperature fatigue crack growth behavior and the micromechanics of fracture.

By cataloging observed microscopic fracture details with stress intensity and temperature we have identified a sequence of microscopic fracture modes that are dependent on input energy (stress intensity) and system energy (temperature, etc.). We have determined that the operative microscopic fracture mode is a function of dislocation mobility and character and the rate of strain energy input. The operative microscopic fracture mode determines fatigue crack growth behavior. To date five of these microscopic fracture modes have been identified. They are (in order of ascending energy):

Low Energy Regime - Room Temperature

- Decohesion (sub microscopic octahedral fracture predominately confined to the matrix phase) - Restricted to PWA 1480
- Submicroscopic octahedral transprecipitate fracture - Restricted to PWA 1484
- Microscopic octahedral fracture (transprecipitate-crystallographic) - Room temperature Region II (of the fatigue crack growth curve)

Intermediate Energy Regime - 427C

- Ancillary decohesion (R=0.1,) (under study)
- Transprecipitate non crystallographic fracture (monoplanar) (R=0.5,)

High Energy Regime - 427C, R=0.5 to 580C R=0.1 K dependent

- Transprecipitate non crystallographic fracture (ancillary)

Other states may exist. Those listed are under study and may be redefined as our understanding of them progresses. They are shown schematically in figure 17.

This complex set of fracture modes exists as a result of the two phase microstructure present in the single crystal alloys. To a large extent this complexity derives from constituent dislocation motion in the matrix and precipitate phases and interactions at the matrix precipitate interface. The driving force behind dislocation motion is input energy (stress/strain in fatigue or stress intensity in fracture). The resistive force , dislocation mobility and or character, is a function largely of temperature. We have found that underlying dislocation dynamics determine (and are mirrored in) observed fracture morphologies. Dislocation trapping in the matrix phase leads to matrix failure. The faulting of octahedral planes under single slip conditions produces octahedral fracture. A proportionate increase in the critical resolved shear stress (CRSS) with temperature results in an increasing crack growth threshold with temperature. The phenomenon stems from the ability of the $L1_2$ structure to deform by thermally activated cube cross slip.

4.3.1: Elevated Temperature Micromechanisms and Transitions

This effort has evolved into a study of the nature of energy-dependent fracture processes and has led us to view the material as a complex energy conversion system. The complexity derives from dislocation dynamics in the constituent phases and interactions with the ordered/disordered interface.

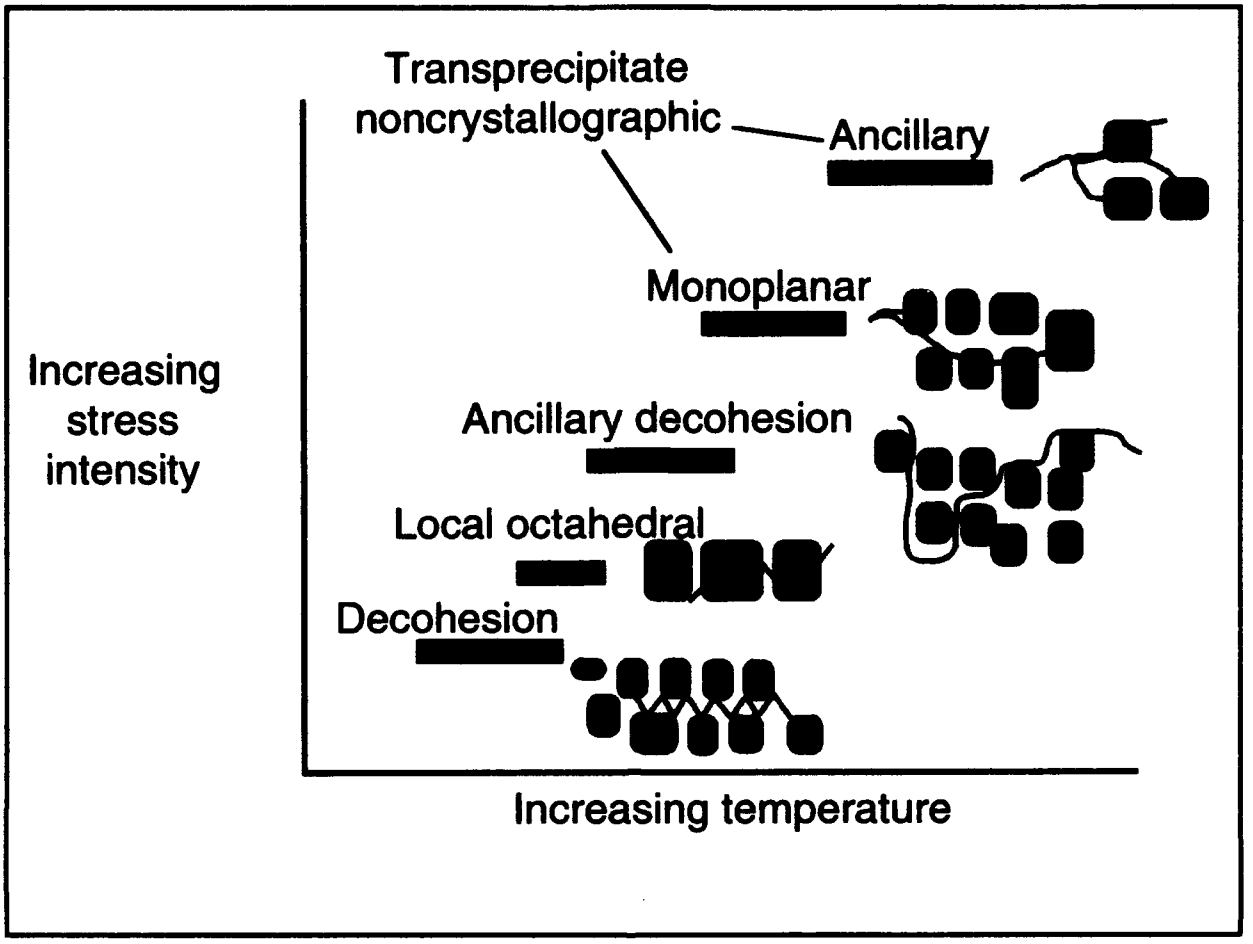

Figure 17: The sequence of energy dependent microscopic fracture modes observed in PWA 1480 and 1484.

The micromechanisms by which the system dissipates imparted mechanical energy, through the development of a free surface, is dependent on the rate of energy input and the system or state energy. System energy refers to a number of temperature dependent phenomena:

- Number of active slip systems
- Increased amplitude of lattice fluctuations
- $\gamma - \gamma'$ mismatch
- Antiphase boundary energy (APBE)
- Superlattice intrinsic stacking fault energy (SFE)

There are others. These affect dislocation mobility and character (octahedral slip, cube cross slip, climb, and bypass.). System energy also encompasses alloy composition and environmental modifiers since they also dictate dislocation mobility. These phenomena determine the micromechanical modes of fracture. Microscopic fracture modes are important because they can effect fatigue crack growth rate, ΔK_{limit} and closure mechanisms such as asperity induced crack tip wedging, for example.

Our assessments of the fracture process have led us to hypothesize that the operative microscopic fatigue crack fracture mode is under some circumstances dictated by an activation energy, set by input and system or "state" energies. They in turn determine the available modes of energy dissipation and the particular mode that will be operative for a given set of service conditions. Transition regions exist between operative fracture modes. Mixed mode fracture occurs in these regions.

The probability of a fracture mechanism transition is important to alternative (statistically based) life modeling approaches [3]. Between initially decohesion and then microscopic octahedral fracture there exists a transition region where mixed mode fracture occurs. A process takes place where increasing input energy results in little or no increase in growth rate. Telesman[4] referred to this region as one "where crack growth rate is independent of stress intensity." The source of this behavior can be hypothesized. While it is true that the cuboidal precipitate structure is uniform and geometrically ordered within the matrix, individual precipitates do exhibit significant deviation from perfect cubes of equal size. This is important since FCG behavior is a function of the operative fracture mode occurring on the precipitate level. The transition in the cuboidal is not a discrete event but rather a K dependent trend due to the variability of a precipitates ability to resist dislocation penetration.

Transitional regions between microscopic fracture modes have also been studied. The transitions have been correlated with ΔK for various stress ratios and temperatures. The following observations have been documented:

1. Numerous microscopic fracture mode transitions from one mode to another have been observed.
2. The available microscopic fracture modes are system energy dependent (primarily alloy composition, environment, and temperature).
3. The operative microscopic fracture mode is input energy dependent (ΔK, K max. or stress ratio).
4. The order in which sequential transitions occur is dependent upon the algebraic sign of the K gradient (constant load or load shedding test).
5. The energy input point, ΔK, at which a transition occurs is independent of K gradient sign.
6. Transition behavior (at constant temperature) is stress ratio, frequency and K dependent. Restated, with system energy constant a transition will be input energy dependent.

   We have observed that in the K gradient test the sequence of a transition can operate in forward or reverse. In an isothermal test, the transition sequence is dependent on the

---

[3] Annis, C and D. P. DeLuca, "Markov Fatigue in Single Crystal Airfoils," ASME 92-GT-95, presented at the International Gas Turbine and Aeroengine Congress and Exposition, Cologne, Germany, June 1-4, 1992.

[4] Telesman, J. and P. Kantzos, "Fatigue Crack Growth Behavior of a Singel Crystal Alloy as Observed Through an In Situ Fatigue Loading Stage," NASA TM 100863, presented at the SAMPE Metals Processing Conference, Dayton, Ohio, Aug. 2-4, 1988.

algebraic sign of the K gradient. Likewise, since these fracture modes are temperature dependent with *K* held constant, we would expect that the sequence of the transition will be determined by the algebraic sign of the temperature gradient. Hence, a paradigm would exist which states that the effect of *K* and *T* on a fracture mode transition are interchangeable. Either parameter can effect a fracture mode transition and the relative amounts of the constituent fracture modes at any point in the mixed mode region of a transition. Therefore, we see the seventh element of our paradigm:

7. The effects of system energy and input energy are interchangeable i.e.. with input energy constant, transitions will be system energy dependent. This is significant in terms of TMF crack growth.

4.3.2: Temperature and Frequency Gradient Crack Growth Test

The increased understanding of the relationship between system and input energy obtained in cataloging micromechanical damage states suggested test techniques that were tailored to produce data on transition behavior and verify the hypothesis described in 4.3.1.

The schematic in Figure 18 shows what might be expected from a T-gradient test where T spans a temperature dependent fracture mode change.

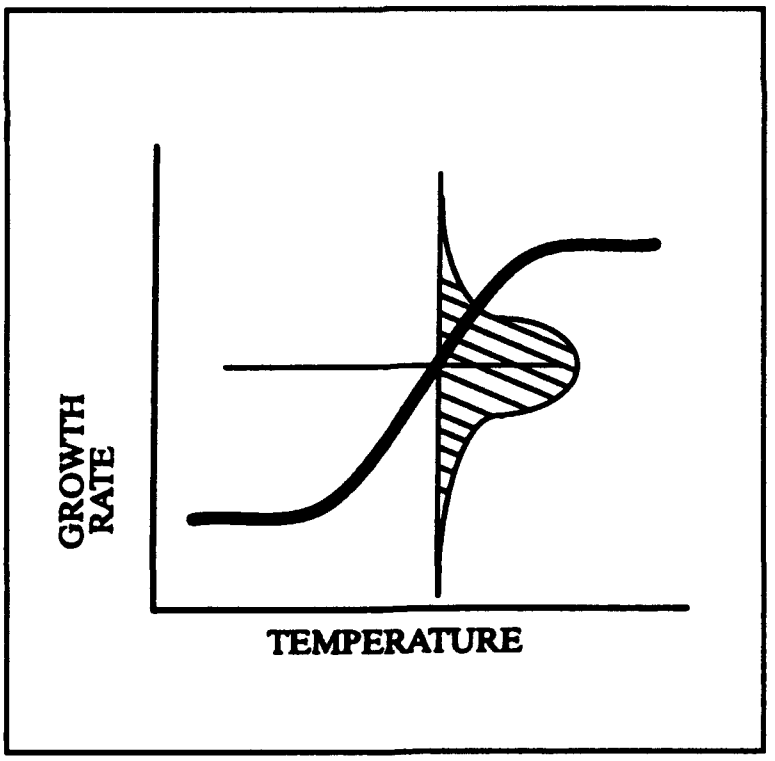

Figure 18: The variability in growth rate is representative of the variability that might be observed with multiple tests. The relationship stems from temperature dependent variation in dislocation mobility.

This figure describes the transition region in terms of the statistical variability that might be expected if tests were conducted on numerous specimens from differing heats of material. This is significant since it implies that the state transition probabilities required by the Markov paradigm are contained in the distribution indicated in the figure. The stochastic component of a fracture mode transition can be inferred because the major source of variability is expected to stem from minor differences in orientation, composition and thermal processing. Composition affects dislocation mobility. Orientation affects the resolved shear stresses on the octahedral planes and thermal processing affects the propensity for cube cross slip (a function of precipitate size).

This test would also provide valuable fatigue crack growth mode information, producing a da/dN vs. temperature plot over the selected temperature range. If the temperature gradient range encompasses a region where a bulk fracture mode transition occurs (Fig. 19), an associated change in fatigue growth rate may occur. This is shown schematically in the da/dN versus temperature plot in Figure 20.

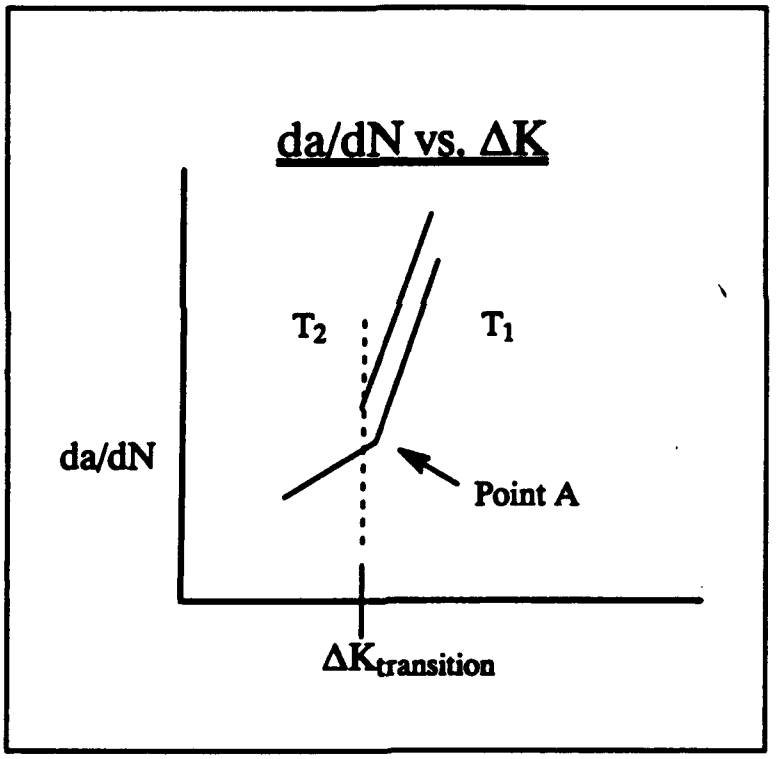

Figure 19: At T_1 a stress intensity dependent fracture mode transition is observed at point A. At $\Delta K_{transition}$ a temperature dependent fracture mode transition exists between T_1 and T_2.

The change in da/dN appears to be proportionate to the relative amounts of the constituent fracture modes present at any point in the transition. An example of these constituents might be microscopic octahedral fracture versus decohesion (cubic) fracture observed on either side of the isothermal K dependent transition that occurs in PWA 1480. However, since the transition is ΔK dependent, a da/dN vs. ΔK plot cannot be produced. Any change in ΔK changes the relative amounts of the constituent fracture modes.

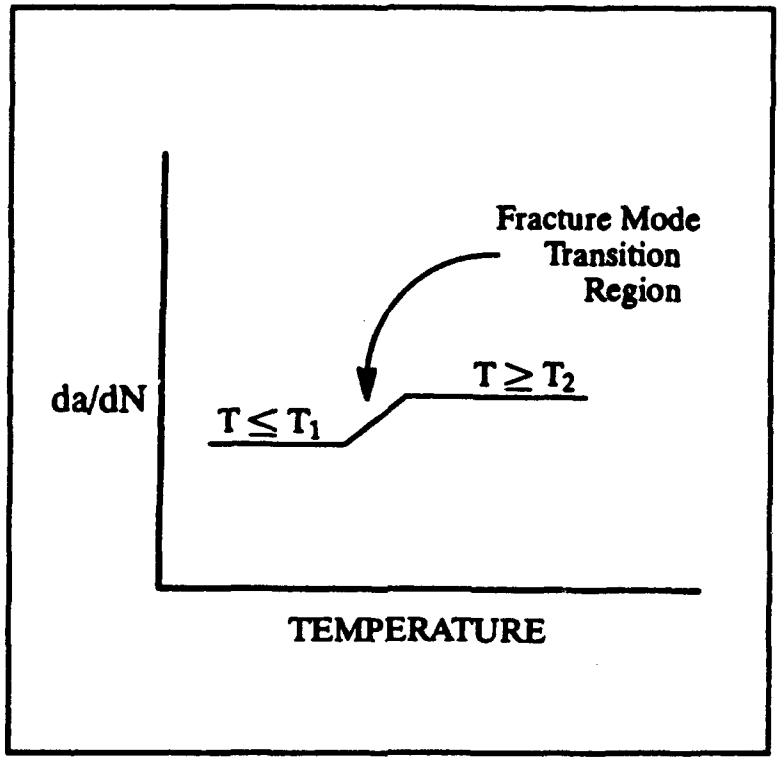

Figure 20: The temperature dependent fracture mode transition described in figure 19 is evaluated in a constant K temperature gradient test at $K_{transition}$ between T_1 and T_2.

Figure 21 describes the preliminary results of a fatigue crack growth test conducted at constant stress intensity ($\Delta K = 3.2$). The initial temperature was 77F. The temperature was increased though the test to a minimum of 600F. The temperature response of FCG at constant ΔK is indicated. FCG is monitored by electric potential drop in these tests. The region where FCG appears to be independent of temperature between approximately 300F and 500 F is revealing since this is a region where fracture mode transition has been documented. This transition was produced by holding input energy constant and changing state energy.

Further experimentation with this technique allowed us to confirm our earlier hypothesis on the interchangeability of state and input energy in producing fracture transitions. As we gathered data for the Markov Paradigm in the early stages of our mechanistic investigation we recognized numerous damage states and documented the importance of transition behavior. It was, however, difficult to envision circumstances where an absorbing state other than failure might occur.

The constant ΔK temperature gradient test described in figure 21 was started at room temperature. As temperature increased, the low energy fracture mode became unavailable.

Successively higher available modes required more energy (ΔK) to drive them; however, ΔK was held constant. Eventually, input energy was insufficient to drive the modes that were available and crack propagation spontaneously arrested.

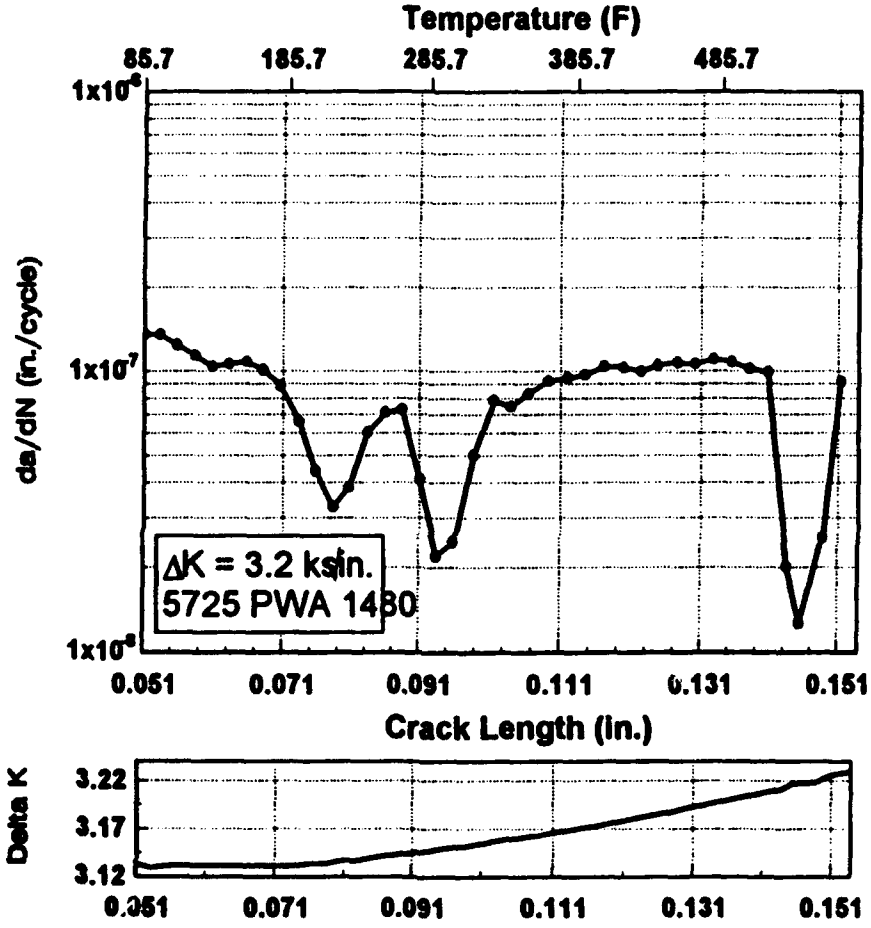

Figure 21: Crack Growth Rate vs. Temperature for PWA 1480, $\Delta K = 3.2 ksi\sqrt{in.}$, Stress Ratio = 0.5, Frequency = 10 Hz from a Temperature Increasing Test Between 77F and 600F at Constant Stress Intensity.

Our interest in transitional behavior led us to recognize the existence of a paradigm describing fracture behavior. This subsequently allowed us to speculate on turbine service conditions where a non-failure absorbing state could occur. The constant ΔK temperature gradient test that produced a system energy dependent fracture mode change resulting in crack arrest. In the domain of the Markov paradigm a transitional state was emerged from. Movement was to a state which could not be departed from, (an absorbing state) crack arrest.

In retrospect, a transition was planned to occur. The transition would be to a state where conditions would not permit emergence. The probability that an absorbing state would be reached was 1 (or as close to 1 as our control of test conditions would permit). Crack propagation spontaneously arrested when an operative low energy fracture mode no longer existed and insufficient input energy was supplied to operate the available higher energy mode.

This set of events has caused us to reconsider component lifing systems that predict thermal mechanical fatigue (TMF) crack growth behavior. Conventional methods of obtaining TMF crack growth data use a one-to-one relationship between load and thermal cycles. We now specify tests where a vibratory component is added to the load cycle in a TMF environment. This more closely simulates blade surface conditions and allows the effect of fracture mode transitions to be observed.

4.3.3: Fracture and Environmental Effects

In our proposal we stated our intent to investigate the effects of pernicious environments such as hydrogen. Our interest in this area stems from experience with single crystals in liquid hydrogen fueled rocket engines. Fatigue and fracture of single crystals in high pressure hydrogen, however, parallels air behavior in a number of aspects.

The presence of atomic hydrogen has been found to have pronounced effects on dislocation dynamics in the cuboidal gamma prime precipitate strengthened superalloys. The chief manifestations are the activation of a normally benign IMQ defect species and an environmentally induced fracture mode transition.

In section 4.1.2.1 we described a microscopic fracture mode transition. The transition was observed in a room temperature fatigue crack growth test of PWA 1480. The *K* dependent transition that occurs in PWA 1480 in the near threshold region results from dislocation trapping in the matrix phase. At higher stress intensities dislocations penetrate precipitates producing fracture along (111) planes.

In high pressure hydrogen the near threshold fracture mode (failure at the matrix-precipitate interface) is operative at very high stress intensities. The change in the deformation mechanism from shearing of the precipitates by $a/2$ <110> dislocation pairs to trapping in the matrix phase has been reported by numerous researchers[5]. Bernenstein[6] and others suggest that hydrogen may affect antiphase boundary (APB) energy of the $L1_2$ superlattice or the misfit strain. The effect is to greatly exacerbate the natural tendency of strain localization and dislocation trapping in the more ductile matrix phase.

---

[5] W. S. Walston, et. al., "The Effect of Hydrogen on the Deformation and Fracture Behavior of a Single Crystal Nickel-Base Superalloy," Hydrogen Effects on Material Behavior, Ed. by N. R. Moody and A. W. Thompson, the Minerals, Metals and Materials Society (1990) 603-612.Walston,etc.

[6] I. M. Bernstein and Dollar, M., "The Effect of Trapping on Hydrogen-Induced Plasticity and Fracture in Structural Alloys," Hydrogen Effects on Material Behavior, Ed. by N. R. Moody and A. W. Thompson, the Minerals, Metals and Materials Society (1990) 603-612.Walston,etc.

Two important points are demonstrated by this comparison:

- Input energy (stress intensity) and state energy (APBE) are interchangeable in producing a fracture mode transition.

- The effect of causing a low energy fracture mode to become operative under high energy conditions is to greatly accelerate crack growth rate.

The air-to-hydrogen fracture mode transition was induced by changing state energy (affecting dislocation mobility) as opposed to input energy (stress intensity) as in the near threshold test.

If we extrapolate room temperature threshold behavior up to Region II of the fatigue crack growth curve, we would predict the effect of causing this "low energy" fracture mode to be operative at high energy conditions. The predicted 100 *X* increase in crack growth rate is accurate and represents an example of a mechanicistally based fracture life prediction approach for PWA 1480 at room temperature in air and hydrogen.

4.3.4: A Shift in Program Direction

We have reassessed our rationale for applying the Markov Paradigm, a statistical technique, to the fatigue and fracture process in single crystals. Our research into the micromechanics of fracture in these materials has greatly enhanced our knowledge of the fracture process. A probabilistic system is especially desirable in the absence of detailed knowledge of the physical processes controlling the events in question. We now can look upon these alloys with a greater appreciation of the underlying physics that dictate fatigue and fracture life than we possess for many of our more conventional alloys. Consequently we have shifted the emphasis of our investigation to describing the necessary elements for a mechanistically based fracture predictive model.

Our ultimate objective will be to formulate a variant of PWA 1480 or PWA 1484 expressly for improved threshold and fatigue crack growth capability based on micromechanical considerations with the aid of atomistic simulations.

SELECTED REFERENCES

1. D. P. DeLuca, B. A. Cowles, H. B. Jones and F. C. Cobia, "Improved Crack Growth in Hydrogen with Modified Precipitate Morphology Single Crystal Nickel," Proceedings, Advanced Earth-to-Orbit Propulsion Technology 1992, Huntsville, Al, May 27, 1992.
2. D. P. DeLuca and B. A. Cowles, "Fatigue and Fracture of Single Crystal Nickel in High Pressure Hydrogen," Hydrogen Effects on Material Behavior, Ed. by N. R. Moody and A. W. Thompson, the Minerals, Metals and Materials Society (1990) 603-612.

REPORT DOCUMENTATION PAGE	1. REPORT NO. FR2198-20	2.	3. Recipient's Accession No.
4. Title and Subtitle FATIGUE IN SINGLE CRYSTAL NICKEL SUPERALLOYS Technical Progress Report			5. Report Date 15 October, 1993 6.
7. Author(s) Charles Annis			8. Performing Organization Rept. No. FR2198
9. Performing Organization Name and Address United Technologies Pratt & Whitney P. O. Box 109600 West Palm Beach, FL 33410-9600			10. Project/Task/Work Unit No. 11. Contract(C) or Grant(G) No. (C) N00014-91-C-0124 (G)
12. Sponsoring Organization Name and Address Office of Naval Research Department of the Navy 800 N. Quincy Street Arlington, VA 22217-5000			13. Type of Report & Period Covered Interim 09/16/91 - 10/15/93 14.
15. Supplementary Notes			

16. Abstract (Limit: 200 words)

This program investigates the seemingly unusual behavior of single crystal airfoil materials. The fatigue initiation processes in single crystal (SC) materials are significantly more complicated and involved than fatigue initiation and subsequent behavior of a (single) macrocrack in conventional, isotropic, materials. To understand these differences is the major goal of this project.

17. Document Analysis a. Descriptors

Fatigue, Fracture, Single Crystal, PWA 1480, PWA 1484

b. Identifiers/Open-Ended Terms

c. COSATI Field/Group

18. Availability Statement	19. Security Class (This Report)	21. No. of Pages
Unlimited	Unclassified	29
	20. Security Class (This Page)	22. Price

(See ANSI-Z39.18) See Instructions on Reverse OPTIONAL FORM 272 (4-77)

* GPO : 1993 0 - 301-526 (8393)